IOP Publishing | Institute of Physics and Engineering in Medicine Physics in Medicine & Biology

Phys. Med. Biol. **59** (2014) 4443–4457 doi:10.1088/0031-9155/59/15/4443

# A microchannel flow model for soft tissue elasticity

**K J Parker**

Department of Electrical and Computer Engineering, University of Rochester, Hopeman Building 203, PO Box 270126, Rochester, NY, 14627-0126, USA

E-mail: kevin.parker@rochester.edu

Received 21 January 2014, revised 8 May 2014
Accepted for publication 17 June 2014
Published 22 July 2014

**Abstract**

A number of advances, including imaging of tissue displacements, have increased our ability to make measurements of tissue elastic properties of animal and human tissues. Accordingly, the question is increasingly asked, 'should our data be fit to a viscoelastic model, and if so which one?' In this paper we focus solely on soft tissues in a functional (non-pathological) state, and develop a model of elastic behavior that is based on the flow of viscous fluids through the extensive network of tissue microchannels in response to applied stress. This behavior can be captured in a 2-parameter model, and the model appears to predict the stress-relaxation behavior and the dispersive shear wave behavior of bovine liver specimens and other soft tissues and phantoms. The relationship of the microchannel flow model to more traditional models is also examined.

Keywords: biomechanics, viscoelasticity, shear waves, dispersion

(Some figures may appear in colour only in the online journal)

## 1. Introduction

The precise viscoelastic properties of soft tissues are important for many fields, from injury protection to surgical devices. In the last 20 years, a major new focus on tissue mechanical properties has arrived with the introduction of the field of 'imaging the elastic properties of tissues', with many diagnostic advances made possible by imaging and quantifying tissue parameters (Parker *et al* 2011). An ongoing debate concerns the most appropriate model to apply to experimental results from elastographic and shear wave speed images. Since there are many different types of tissues and since all tissue models are only approximations, there is ample room for different approaches (Delingette 1998, Liu and Bilston 2000, Walker *et al* 2000, Humphrey 2003, Bercoff *et al* 2004, Catheline *et al* 2004, Chen *et al* 2004, Gennisson *et al* 2006, Samani *et al*

  

2007, Chen *et al* 2009, Giannoula and Cobbold 2009, Chen *et al* 2013a,b). The most common viscoelastic models include the Maxwell (series spring and dashpot), the Kelvin-Voigt (parallel spring and dashpot), and more elaborate configurations including the Zener or Standard model, progressing to the many elements of the Maxwell-Weichert model (Fung 1981, Carstensen and Parker 2014). There are also models that invoke fractional order integrals and derivatives, and the Kelvin-Voigt Fractional Derivative (KVFD) model has been applied to a number of experimental results from different tissues (Caputo 1967, Bagley and Torvik 1983, Suki *et al* 1994, Taylor *et al* 2001, Kiss *et al* 2004, Robert *et al* 2006, Zhang *et al* 2007).

In this paper we derive a model based on extracellular fluid flow in the microvasculature and related channels, aiming for the simplest and most appropriate approximation for soft tissues. By 'soft tissues' we mean relatively isotropic and homogeneous tissues such as the liver, the prostate, and the thyroid in their normal state. By 'model' we mean an analytical approximation that closely captures and predicts the small amplitude response of tissue to applied stress or strain. We are not considering large strains and nonlinear behavior. The following considerations guide the development of this paper:

(1) agreement with observed behavior. A valid model must predict some reasonable range of experimental measurements. In this paper we are specifically concerned with two different sets of small-strain measurements:

- stress relaxation measurements
- shear wave speed and dispersion measurements

These are commonly reported measurements and they should be mutually consistent with an accurate model.

(2) Philosophy of a preferred model. When choosing between different models that match the observed behavior with reasonable accuracy, the one with the fewest parameters is the preferred and canonical model. The preference and priority for the most simple model, including the fewest parameters, is succinctly captured by Ockham's razor (Britannica 2013). Furthermore, there is a practical reason to prefer a model with 2 or 3 parameters as opposed to 6 or more parameters. Experimental data over a limited range of time or frequency, in the presence of noise, is commonly input to a curve-fitting routine to derive the model parameters. The confidence in the resulting best fit parameters is weakened as the number of simultaneous unknowns is increased. Finally, when choosing among competing models with equally few parameters, the model with parameters that can be directly linked to tissue structure, composition, and architecture, is preferred.

In this paper, we attempt to meet the guiding principles above by deriving a model which in its simplest form has two parameters linked to the fluid outflow from the distribution of microchannels and microvasculature in soft tissues such as the liver. We specifically aim to predict the stress relaxation results and shear wave dispersion results shown in figure 1.

These results were selected by Drs M Zhang, L Taylor, and B Castaneda in our lab after their experience with measurements of hundreds of samples from livers, prostates, and other soft tissues and phantoms (Taylor *et al* 2001, Taylor 2002, Taylor *et al* 2002, Zhang *et al* 2007). As such, we believe these examples of stress relaxation and shear wave speed versus. frequency are representative of the stress-strain behavior of healthy soft tissues under conditions that exist in many *ex vivo* elastographic and shear wave imaging techniques. Any valid model must therefore be capable of demonstrating the time-domain and frequency-domain behavior shown in these figures.

The organization of this paper begins with a consideration of the stress-strain relations for a tissue with multiple microchannels. Once established, the second section summarizes

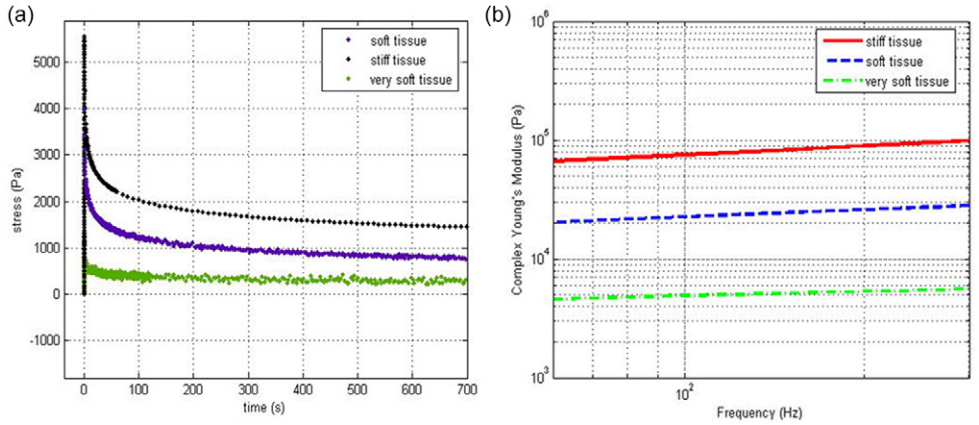


**Figure 1.** A diagram of (*a*) the typical stress relaxation curves obtained from cylindrical cores of different soft tissues at 5% strain, and (*b*) the typical frequency dependent Young's moduli of soft tissues with different stiffness, as predicted from (*a*) and as verified from independent shear wave measurements (see Zhang *et al* (2007) reproduced with permission from Elsevier).

key attributes of the KVFD model. The third section compares the microchannel flow model against the KVFD model, in order to reconcile similarities and differences. A test on treated liver samples is presented for comparison against theory. Finally, some practical issues and limitations are discussed.

## 2. Theory

### *2.1. Microchannel flow*

Consider a block of liver tissue (figure 2), comprised of a fine-scale interlocking of hepatic cells, connective tissue, and a variety of fluid channels including billary, capillary, and lymphatic.

As a structural element, we isolate a perfect cube, support it at the base, and subject it to uniaxial loading in the $x$-direction (figure 3).

Using conventional notation, $\sigma_x$ is the stress and $\epsilon_x$ the engineering strain in the $x$-direction. If a steady force $F$ is applied to the upper surface of area $A$, then $\sigma_x = {F}/{A}$. We assume that the idealized tissue block has an elastic component $E$ and that stress is approximately uniform over the element. In the case of a pure elastic response, the element would follow Hooke's Law, $\sigma_x = E\epsilon_x$. Now consider the inclusion a small fluid microchannel (figure 2). If the fluid within a microvessel of length $L$ experiences a pressure drop $\Delta P$, then under Poiseuille's Law for incompressible fluids in pipes, a volumetric flow rate $Q$ will result (Sutera 1993).

$$Q = \frac{\Delta P \pi r^4}{\eta 8 L} \tag{1}$$

where $r$ is the radius of the microvessel, $\eta$ is the viscosity of the fluid, and $L$ is the length of the vessel segment. We then assume that the pressure $P_{in}$ within the sample and microchannel interior is proportional to $\sigma_x$, and is zero outside the sample. Then the pressure drop is simply:

$$\Delta P \cong (P_{in} - 0) \cong C_1 \sigma_x \tag{2}$$

where $C_1$ is a constant of proportionality. Combining equation (1) and (2) gives

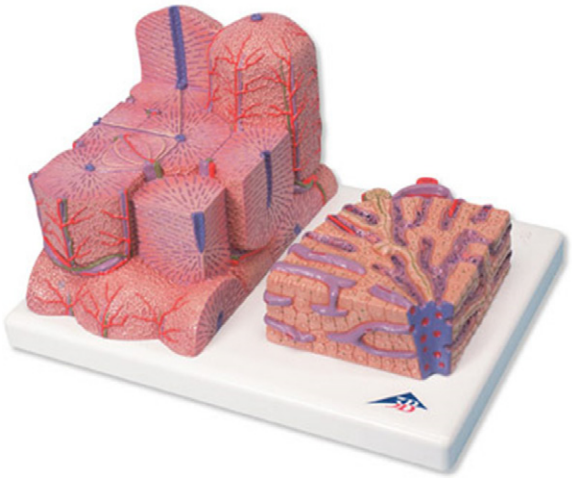

**Figure 2.** Magnified views of liver microchannels in 3D. This microanatomical liver model is rendered by 3B Scientific (reproduced with permission (www.a3bs.com/)).

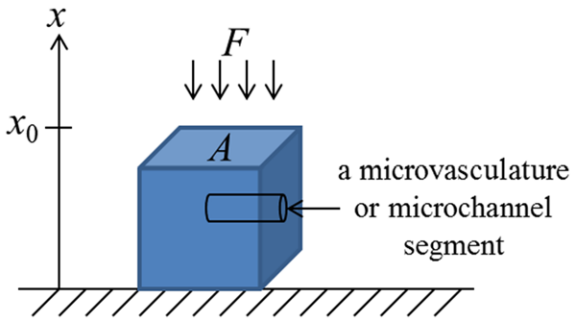


**Figure 3.** Model of stress and flow on an idealized cube of soft tissue.

$$Q = \frac{C\sigma_x r^4}{\eta} \tag{3}$$

where $C$ is a constant that incorporates all previous constant terms. Here we assume the fluid exits the free boundary shown in figure 3. The loss of fluid volume will result in a loss of volume in of the original cube, and this can be related to the change in height of the block under compression. Assuming we can, to first order approximation neglect the change in cross section area $A$ caused by the lateral strain, the volume change from the loss of fluid from the sample must be accounted for by a decrease in the $x$-dimension, or strain $\varepsilon$. Thus,

$$\frac{d\varepsilon_x}{dt} = \frac{Q}{A_0 x_o} = \frac{C\sigma_x r^4}{\eta A_0 x_0} \tag{4}$$

or

$$\sigma_x = \eta\left(\frac{A_0 x_0}{Cr^4}\right)\frac{d\varepsilon_x}{dt} \tag{5}$$

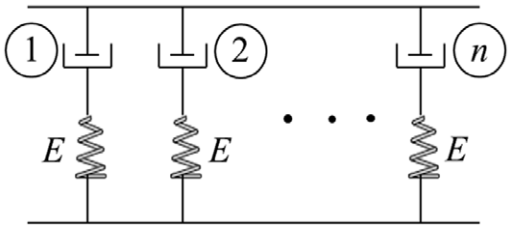


**Figure 4.** Parallel elements.

Note that this resembles the equation for a simple dashpot and, furthermore, the basic proportionality between $d\varepsilon/dt$, $Q$, and $\sigma$ could alternatively be derived from Darcy's Law, assuming a porous material. This will be reconsidered later. Now combining elastic and fluid outflow strains as additive leads to a Maxwell model of a series spring and dashpot, where the stress relaxation (SR) curve is a simple exponential decay. If $\varepsilon(t) = \varepsilon_0 \text{UnitStep}(t)$, then

$$\sigma_{SR}(t) = \varepsilon_0 E \mathbf{e}^{-t/\tau} \text{ for } t \geq 0. \tag{6}$$

where the time constant $\tau = \eta A x_0 / ECr^4$. It should be noted that the single time constant exponential decay is not capable of matching soft tissue stress relaxation responses, nor the frequency responses (figure 1).

Now assume there are multiple microchannels of unequal radius $r_n$ and therefore unequal flow rates $Q_n$. In this case, if each contributes to the stress relaxation at their respective time constant $\tau_n$, then the simplest model for this looks like a parallel set of Maxwell elements (figure 4).

This configuration of multiple parallel elements and an optional single spring element is the generalized Maxwell-Weichert model (Fung 1981). Generally, we can write the stress relaxation solution for $N$ Maxwell elements as

$$\sigma_{SR}(t) = \sum_N A_N \mathbf{e}^{-t/\tau_N} \tag{7}$$

where $A_N$ are the relative strengths of the components with characteristic relaxation time constant $\tau_N$. In the limit, as we allow a continuous distribution of time constants $\tau$, the summation becomes an integral and $A(\tau)$ is the relaxation spectrum, which can be either discrete or continuous, depending on the particular medium under study (Fung 1981). Given a material's $A(\tau)$ we can write:

$$\sigma_{SR}(t) = \int_0^\infty A(\tau) \mathbf{e}^{-t/\tau} d\tau \tag{8}$$

Now consider a specific power law distribution:

$$A(\tau) = A_0 \tau^{-b}; \quad 1 < b < 2 \tag{9}$$

One rationale for introducing this function is that the power law distribution is frequently found to describe fractal systems in nature and biology (West *et al* 1999). Specifically, power law distributions have been observed in measures related to branching vasculature, including

normal and pathological circulatory systems (Gazit *et al* 1997, Risser *et al* 2007). Substituting equation (9) into equation (8) and solving yields the solution:

$$\sigma_{SR}(t) = A_0 \cdot t^{1-b}\Gamma[b-1] \quad \text{for} \quad 1<b<2, \quad t>0 \tag{10}$$

where $\Gamma$ is the Gamma function. The stress relaxation response is characterized by $1/t^{b-1}$ decay for $t>0$. For values of $1<b<2$ this tends to have a sharp initial drop and then a slow asymptotic decay. The derivative of the step response yields the impulse response, which defines the basic elastic transfer function for the material. If $\varepsilon(t) = \varepsilon_0\delta(t)$ „ then

$$\sigma_i(t) = \varepsilon_0 A_0 \Gamma[b-1][(1-b)\,t^{-b}] \quad \text{for} \quad 1<b<2, \quad t>0 \tag{11}$$

For simplicity, let $a = b-1$ and given the restriction on $1<b<2$, then $0<a<1$. The impulse response normalized by $\varepsilon_0$ is

$$\sigma_i(t) = A_0\Gamma[a][-a/t^{(a+1)}] \quad \text{for} \quad t > 0 \tag{12}$$

The Fourier transform of equation (12) is:

$$E(\omega) = \frac{A_0}{\sqrt{2\pi}}\Gamma[a]\,\Gamma[1-a]\,\mathrm{Abs}[\omega]^a\left(\cos\left[\frac{a\pi}{2}\right] + \mathrm{jSign}[\omega]\sin\left[\frac{a\pi}{2}\right]\right) \tag{13}$$

where $j = \sqrt{-1}$. This response is dominated by the steady increase with frequency to the power of $a$.

Let us recap the derivations. If a tissue has a distribution of microchannels leading to a power law relaxation spectrum $A(\tau) = \tau^{-b}$, then the stress relaxation response will show a $\sigma_{SR} \cong t^{1-b} = 1/t^a$ response. The tissue stress-strain transfer function in the frequency domain, $E(\omega)$, will have an $|\omega|^{b-1} = |\omega|^a$ dependence. For example, let $b = 5/4$ then $A(\tau) = 1/\tau^{5/4}$ and, thus, $\sigma_{SR} \cong 1/\tau^{1/4}$ and $|E(\omega)| \cong |\omega|^{1/4}$. These values happen to closely match soft tissue response (see figures 1(*a*, *b*), compared to 5(a, b).

The transfer function $E(\omega)$ of tissue samples was cross checked by Zhang *et al* (2007) in two ways. First, curve fitting of $\sigma_{SR}(t)$ was performed and the KVDF Fourier transform relations applied to plot $E(\omega)$. These equations will be reviewed in the next section. The second way of estimating $E(\omega)$ was from measurements of shear wave phase velocity $c_{ph}$ at discrete frequencies. For a lossless plane shear wave in a homogeneous, nearly incompressible elastic medium we find that $c_{ph} = \sqrt{E/3\rho}$ where $\rho$ is density (Graff 1975, Parker *et al* 2011, Carstensen and Parker 2014), and in this simple case the speed is constant over any frequency band. More generally, when $E$ is frequency dependent and complex, the complex wave number $\hat{k}$ is given by (Blackstock 2000, Carstensen and Parker 2014):

$$\hat{k} = \frac{\omega}{\sqrt{\frac{E(\omega)}{3\rho}}} = \beta - j\alpha, \quad \text{where } \beta = \frac{\omega}{c_{ph}} \tag{14}$$

and $\alpha$ is the attenuation, taken from the real and imaginary parts of the $\omega/\sqrt{E(\omega)/3\rho}$ term, respectively. For the microchannel flow model, if $|E(\omega)| \propto \omega^{b-1}$, then $c_{ph}^2(\omega) \propto \omega^{b-1}$ also. This was the experimental observation of Zhang *et al* (2007).

Experienced readers will recognize that the 2-parameter microchannel flow model's behavior resembles a simplified KVFD model. In the next section we review the 3-parameter KVFD which indeed reduces to the microchannel model for the case where the parallel spring $E_0$ is set equal to 0. However, the key difference lies in derivation, as the microchannel flow model

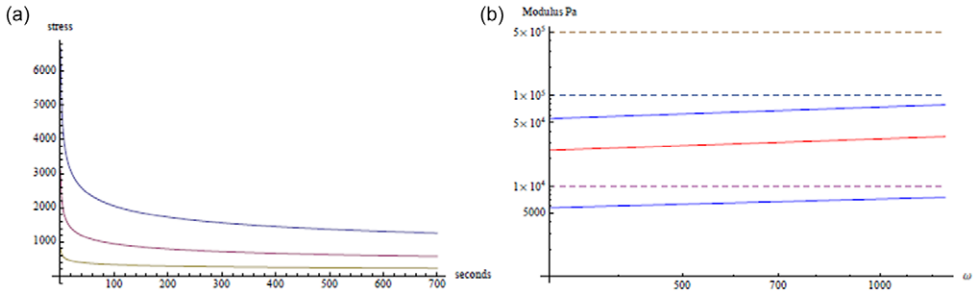


**Figure 5.** In (*a*) the stress relaxation functions $(6500/t^{1/4})(3000/t^{1/4})(800/t^{3/16})$ on a similar scale as figure 1(*a*). In (*b*) the Fourier transform magnitude of the three functions (solid lines), shown on the same scale as figure 1(*b*). The functions closely match observed behavior of soft tissues.

is constructed without invoking *a priori* mathematical definitions of fractional derivatives or fractional transforms. Instead it is derived from fluid flow distribution of the relaxation spectrum, linked to tissue architecture.

### *2.2. The Kelvin-Voight fractional derivative model*

Fractional derivatives describe some systems that contain a broad distribution of relaxation times (Sokolov *et al* 2002). The Kelvin-Voight fractional derivative (KVFD) model is a generalization of the Kelvin-Voight (KV) model. Caputo (1967) introduced a fractional calculus Kelvin-Voigt model that consists of a spring in parallel with a dashpot where the stress in the dashpot is equal to the fractional derivative of order $a$ of the strain. Koeller (1984) derived the stress relaxation function, with a time dependence $t^{-a}$ in the function for the KVFD model. Later, Bagley and Torvik (1983) described molecular theories that predicted the macroscopic behavior of some viscoelastic polymers and established a link between those theories and the empirical approach from fractional derivative models. Suki *et al* (1994) argued that the molecular theories derived for polymers may also apply to soft tissues because biological tissues consist of long flexible biopolymers. They used the fractional calculus in biomechanics and discussed the utility of the single fractional dashpot to the KV model. A number of papers have explored the power law behavior of waves in attenuating media (Szabo 1994, Szabo 1995, Szabo and Wu 2000, Chen and Holm 2003, Sushilov and Cobbold 2004, Holm *et al* 2013, Holm and Nasholm 2014). Szabo and Wu (2000) described a frequency-dependent power law for ultrasound attenuation in soft tissues, suggesting that many soft tissues can be modeled by a generalized KV model, where the dashpot is replaced by a convolution operator. Taylor *et al* (2002) further investigated the KVFD model by fitting the liver relaxation data to this model. Dynamic testing was performed by Kiss *et al* (2004) on canine liver, and the data were fitted to both the KVFD model and the KV model. After comparison of the curve fitting results of the two models, they concluded that the KVFD model had better agreement with the experimental data than the KV model.

In the KV model, stress in the dashpot is equal to the first derivative with respect to time of the strain. The KVFD model consists of a Hookean spring in parallel with a fractional derivative dashpot (figure 6).

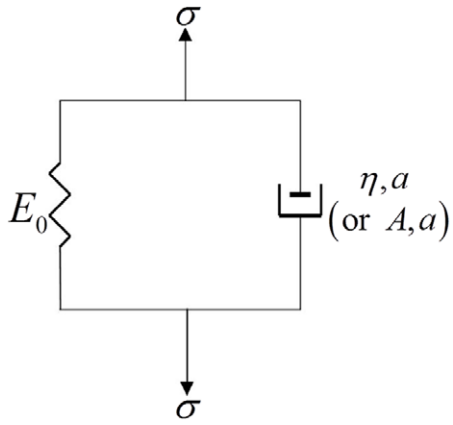


**Figure 6.** The KVFD model.

The stress in the dashpot is equal to the fractional derivative of the strain. The KVFD model contains three parameters: $E_0$, $\eta$, and $a$, where $E_0$ refers to the relaxed elastic constant, $\eta$ refers to the viscoelastic parameter, $a$ is the order of fractional derivative. The relationship between stress and strain in the KVFD model is given by the following constitutive differential equation:

$$\sigma(t) = E_0\varepsilon(t) + \eta D^a[\varepsilon(t)] \tag{15}$$

where $\sigma$ is stress and $\varepsilon$ is strain.

$D^a[\,]$ is the fractional derivative operator defined by (Mainardi 1996)

$$D^a[x(t)] = \frac{1}{\Gamma(1-a)}\int_0^t \frac{x'(\tau)}{(t-\tau)^a}d\tau \tag{16}$$

where $x'(t)$ refers to the first derivative of the function $x(t)$ with respect to $t$. For the KVFD model we restrict that $0<a<1$.

*2.2.1. Stress relaxation.* To derive the stress relaxation response of the KVFD model we follow the derivation of Zhang *et al* (2007). The applied strain is modeled as a ramp of duration $T_0$, followed by a hold period of constant strain $\varepsilon_0$ (Taylor 2002). So the strain function is:

$$\varepsilon(t) = \begin{cases} (t/T_0)\,\varepsilon_0 & \text{if} \quad 0<t<T_0 \\ \varepsilon_0 & \text{when} \quad t\geq T_0 \end{cases} \tag{17}$$

By taking the Laplace transform of the constitutive equation (15) and equation (17), we get

$$\sigma(s) = E_0\varepsilon(s) + \eta s^a\varepsilon(s) \tag{18}$$

$$\varepsilon(s) = \frac{\varepsilon_0}{s^2T_0}(1 - \mathbf{e}^{-sT_0}) \tag{19}$$

where $s$ is the Laplace domain variable. We substitute equation (18) into equation (19) and obtain

$$\sigma(s) = E_0\frac{\varepsilon_0}{s^2T_0}(1 - \mathbf{e}^{-sT_0}) + \eta\frac{\varepsilon_0}{s^{2-a}T_0}(1 - \mathbf{e}^{-sT_0}) \tag{20}$$

Then, inverse Laplace transform is applied to both of the terms in equation (20)

$$\sigma(t) = E_0 \frac{\varepsilon_0}{T_0}(tu(t) - (t-T_0)\,u(t-T_0)\,) + \eta \frac{\varepsilon_0}{\Gamma(2-a)\,T_0}(t^{1-a}u(t) - (t-T_0)^{1-a}\,u(t-T_0)\,) \tag{21}$$

where $u(\,)$ is the unit step function. Therefore, during the hold period ($t \geq T_0$) of the stress relaxation curve, the response of a material exhibiting KVFD behavior is

$$\sigma_{SR}(t) = E_0\varepsilon_0 + \eta \frac{\varepsilon_0}{\Gamma(2-a)\,T_0}(t^{1-a} - (t-T_0)^{1-a}\,) \tag{22}$$

*2.2.2. Frequency response: the complex Young's modulus.* The frequency-domain response can be obtained from the time-domain response and has a frequency-dependent complex-valued Young's modulus. Taking the Fourier transform of the constitutive equation (15) yields

$$\sigma(\omega) = E_0\varepsilon(\omega) + \eta(j\omega)^a\,\varepsilon(\omega) \tag{23}$$

where $\omega$ is radian frequency and the radian frequency is restricted to be positive, i.e., $\omega \geq 0$. The complex modulus as a function of frequency $E(\omega)$ is then obtained by

$$E(\omega) = \frac{\sigma(\omega)}{\varepsilon(\omega)} = \left[E_0 + \eta\cos\left(\frac{\pi a}{2}\right)\omega^a\right] + j\left[\eta\sin\left(\frac{\pi a}{2}\right)\omega^a\right] \tag{24}$$

The magnitude of $E(\omega)$ can be expressed as

$$|E(\omega)\,| = \sqrt{E_0^2 + 2E_0\eta\cos\left(\frac{\pi a}{2}\right)\omega^a + \eta^2\omega^{2a}} \tag{25}$$

From equation (24) we get the storage modulus, $E'(\omega)$, which is the real part of the complex modulus, and the loss modulus, $E''(\omega)$, which is the imaginary part.

$$E'(\omega) = E_0 + \eta\cos\left(\frac{\pi a}{2}\right)\omega^a \tag{26}$$

$$E''(\omega) = \eta\sin\left(\frac{\pi a}{2}\right)\omega^a \tag{27}$$

The storage modulus is related to the elasticity of the soft tissue, whereas the loss modulus is related to viscoelasticity.

### *2.3. Comparison of models*

Here we examine the relationship between the KVFD and the microchannel flow model solutions for stress relaxation and for shear wave dispersion. The key difference is the KVDF spring $E_0$. It is germane to point out that Zhang *et al* (2007) and Taylor (2002) found that the vast majority of their soft tissue stress relaxation responses, when curve fit to the KVFD model, found $E_0$ very close to zero. In other words, the parallel spring does not seem to be a necessary or required element for many soft tissues. Here we are open to the possibility of $E_0$ being useful for other types of tissues including fibrotic tissues, but the simplest model without $E_0$ has some range of applicability. Accordingly, if we set $E_0$ equal to 0 in the KVFD model, and examine the frequency dependence of $E(\omega)$ in equation (24), this is shown to be

equal to $E(\omega)$ derived from the microchannel flow model in that they both increase with frequency to the power of $a$ and have a loss tangent independent of frequency.

Now comparing the stress relaxation responses, the microchannel flow model predicts a response that, according to equation (10), decays as $t^{(1-b)}$ or $1/t^a$ for $t>0$. The KVFD response as derived in equation (22) appears to be slightly different, even with $E_0$ set equal to 0. However, this equation is derived for a practical stress relaxation experiment where a finite ramp of strain is applied over a short period $T_0$, as compared with an idealized unit step with an instantaneous and discontinuous jump in strain.

If we assume $E_0$ is 0 and $T_0$ is small, then equation (22) becomes

$$\sigma_{SR}(t) \propto \frac{(t^{(1-a)} - (t - T_0)^{(1-a)})}{T_0} \tag{28}$$

Consider the definition

$$\frac{df(t)}{dt} \cong \lim_{T_0 \to 0} \frac{(f(t) - f(t - T_0))}{T_0} \tag{29}$$

written as a first backward difference. Comparing equation (28) and (29), we let $f(t) = t^{(1-a)}$ and assuming the ramp period $T_0$ is small, and taking the derivative of $t^{(1-a)}$, we have

$$\sigma_{SR}(t) \propto \frac{(1 - a)}{t^a} \text{for } t > T_0 \tag{30}$$

which is similar to the microchannel flow model, equation (10).

## 3. Discussion

In this section some practical issues are addressed.

(1) Avoiding singularities. The more empirical-minded researchers prefer to avoid mathematical singularities which cannot be achieved or measured experimentally, or are difficult to handle in analytical operations such as transforms and convolutions. The microchannel model has a singularity in the relaxation spectrum in $A(\tau)$ at $\tau = 0$, and a singularity in the stress-relaxation response at $\sigma_{SR}(t)$ at $t = 0$. A simple way to avoid these is to limit the lower range of the relaxation spectrum to some small time constant $\tau = l$. Then

$$\sigma_{SR}(t) = \int_l^\infty \left(\frac{A_0}{\tau^b}\right) \mathbf{e}^{-t/\tau} d\tau = A_0 \left[\Gamma[a] - \Gamma\left[[a], \frac{t}{a}\right]\right] \frac{1}{t^a} \text{ for } t > 0 \text{ and } a > 0 \tag{31}$$

where $a = b - 1$ and $\Gamma\left[[a], \frac{t}{a}\right]$ is the incomplete Gamma function. The subtraction of the Gamma terms in brackets yields a zero at $t = 0$, sufficient to create a finite value of $\sigma_{SR}(t = 0)$. The effects of this practical adjustment is only visible for small $t$ in $\sigma_{SR}(t)$, but it comes at the expense of introducing a third parameter, $l$. It should be noted that the integral in equation (31) could have a finite upper limit $l_2$ instead of infinity. This would represent a tissue structure in which both upper and lower limits of the relaxation spectrum are known. This solution has two incomplete Gamma functions and is given in table 1. However, by referring again to Ockham's razor, we prefer to not invoke an extra parameter unless it is necessary.

Another way to eliminate the singularity from the stress relaxation curve at the origin is to consider the more practical solution of equation (22) where the strain function is a continuous,

**Table 1.** Microchannel models in increasing order of complexity.

| Parameters | Stress relaxation formula | Comments |
|---|---|---|
| Two: $A$, $a$ | $A\Gamma[a]\,/\,t^a$ | Microchannel flow model |
| Three: $A$, $a$, $l$ | $A[\Gamma[a]-\Gamma[a,\,(t/l)\,]\,]\,/\,t^a$ | Microchannel flow with lower limit $l$ of relaxation spectrum |
| Three: $A$, $a$, $E_0$ or $\eta$, $a$, $E_0$ | $E_0 + A\Gamma[a]/t^a$ | KVFD or microchannel flow with parallel $E_0$ |
| Four: $A$, $a$, $l_1$, $l_2$ | $A[\Gamma[a,\,(t/l_2)\,]-\Gamma[a,\,(t/l_1)\,]\,]\,/\,t^a$ | Microchannel flow with lower limit $l_1$ and upper limit $l_2$ of the relaxation spectrum |
| Four: $A_1$, $a_1$, $A_2$, $a_2$ | $A_1\Gamma[a_1]\,/\,t^{a_1}+A_2\Gamma[a_2]\,/\,t^{a_2}$ | Microchannel flow in polymer viscoelastic tissue |
| Five or more | Combinations of above | Combinations of above |

short ramp applied over $T_0$ and then held, as opposed to an idealized discontinuous step function. In that case, the stress relaxation solution for $t > T_0$ is finite everywhere and can be linked to the power law behavior of $1/t^a$ for small $T_0$ as explained in equations (28) through (30).

(2) Compatibility with polymer models. The microchannel flow model has been derived assuming an elastic tissue medium, and yet the solid tissue components of protein, collagen, and elastin could exhibit their own viscoelastic behavior. In fact many polymer models predict power law relaxation behavior (Van Oene 1978, Grizzuti *et al* 2000), and so this raises the possibility of a more complicated response of tissue. In the simplest case, consider a stress relaxation response comprised of two equal parts, a $1/t^{(1/4)}$ component from a microchannel relaxation spectrum and a $1/t^{(1/2)}$ from a polymer tvpe of relaxation. Mathematically, it is not the case that these two functions average to a $1/t^{(1/3)}$ composite result.

However, for stress relaxation times around 1 – 10 s, it is very difficult to distinguish between these functions, and careful precision at very small values or large values of $t$ are required to confidently make the distinction. Because of these considerations, we postulate that the microchannel model may incorporate viscoelastic effects of the tissue matrix that are similar enough to fall within the general model of a relaxation spectrum with power law distribution.

(3) Time-temperature superposition. It is an empirical fact that some tissue and biomaterial viscoelastic properties obey a model of time-temperature superposition (Chan 2001, Doyley *et al* 2010). The model is based on consideration of relaxation mechanisms and the theoretical temperature dependence of the relaxation mechanisms. It is germane to point out that in the flow of fluids, including blood plasma, viscosity is temperature dependent and therefore the time constants and relaxation spectrum of the microchannel model will depend on temperature and can therefore be consistent, at least in principle, with the general predictions of time-temperature superposition models.

(4) Poroelastic models. Under Darcy's law (Swartz and Fleury 2007) a pressure gradient across a porous material sets up a volumetric flow rate $Q$. The proportionality includes the permeability constant of the material $\kappa$ instead of the single vessel radius used in the initial consideration of a medium and Poiseuille's law in equation (5). The permeability is a macroscopic measure of the ease at which fluid can flow within the matrix in response to a pressure gradient; as such it incorporates the distribution of pores within the material. While the characterization of porous media has a long history (de Boer 1996), important milestones include developments by Biot (1941, 1962), the biphasic model by Mow *et al* (1980), (Armstrong *et al* 1984) for cartilage, and a poroviscoelastic model proposed by Mak (1986). Poroelastic models have been applied to many tissues, and linked to elastographic imaging techniques (Mow *et al* 1984, Miller and Chinzei 1997, Ehlers and Markert 2001, Konofagou *et al* 2001, Righetti *et al* 2004, Berry *et al* 2006, Cheng and Bilston 2007,

Righetti *et al* 2007, Swartz and Fleury 2007, Perrinez *et al* 2009, Perrinez *et al* 2010). If we assume a porous model for figure 3, then the applied stress still produces a proportional flow rate $Q$, thus the remaining derivation of $d\varepsilon_x/dt$ to the classic spring-dashpot result is similar. In order to invoke a relaxation spectrum under a porous model, we would then need to hypothesize a power law distribution of permeability within the tissue sample; that is, networks of larger and smaller pores that lead to a distribution of permeability constants. It would be useful to see if solutions to uniaxial compression of a poroelastic material (Armstrong *et al* 1984, Konofagou *et al* 2001) can be compatible with the microchannel flow model, but this will require further research.

(5) The relaxation spectrum. From equation (5) and (6) we conclude that the time constant $\tau$ is proportional to $1/r^4$ where $r$ is the vessel radius. But $A(\tau)$ is proportional to $1/\tau^b$. Thus the smallest time constants corresponding to the largest vessels are strongly weighted. It may be that additional scale factors involving average length, number, viscosity, and stress concentration effects as a function of channel size play a role in generating the overall $A(\tau)$ relaxation spectrum. This remains open to further research.

(6) Limits of the model. The model does not include inertial effects, as in the acceleration or second derivative of time terms that would be part of a complete treatment of the response of the fluid to rapid changes in pressure. However typical frequencies used in elastographic shear wave configurations are below 500 Hz or even below 100 Hz in larger organs. Inertial effects could play a role, but the strong effects of viscosity in narrow channels makes it likely that the second order system would be highly overdamped. Again resorting to Ockham's razor, inertial effects would add another parameter yet they should not be employed unless required to fit experimental results over the range of conditions being observed. Another key limitation of the model is that under steady state stress or strain over time, the fluid in vessels will be expelled and the vessels will collapse. Any effects of collapse and post-collapse are clearly not included in the model, so long duration stress relaxation measurements may require additional terms. Furthermore, as stated in the introduction, only small strain and linear behaviors have been considered for 'soft tissues', so this model would not apply where nonlinear, large strain, anisotropic, or long duration conditions are found. The use of this model *in vivo* entails additional considerations including the contributing factors of arterial and interstitial pressure. A complete solution for loading of *in vivo* organs must include boundary conditions and tractions as well as the microchannel model as a constitutive relation.

## 4. Conclusion

The microchannel model is developed from consideration of the flow of fluids through microvasculature and microchannels in soft tissue. The derivation, along with a power law relaxation spectrum, leads to a two parameter model of tissue, $A_0$ and $a$ of equation (12) and (13), capable of modeling the frequency domain measurements and the stress relaxation measurements of soft tissues. This resembles the KVFD model; however, the microchannel flow model is derived from linear superposition using a relaxation spectrum that is linked to the natural distribution of tissue architecture, specifically fluid channels within the tissue elastic matrix. The hierarchy of models suggested in this paper is listed in table 1 for reference, yet the preference remains for the lowest order model capable of characterizing the particular soft tissue under evaluation.

## Acknowledgements

This paper was motivated in large part by the penetrating insights and queries of Professor Ed Carstensen. Additional expertise and advice from Professor Sheryl Gracewski is gratefully

recognized. This work was supported by the University of Rochester Department of Electrical and Computer Engineering.

## References

Armstrong C G, Lai W M and Mow V C 1984 An analysis of the unconfined compression of articular cartilage *J. Biomech. Eng.* **106** 165–73

Bagley R L and Torvik P J 1983 A theoretical basis for the application of fractional calculus to viscoelasticity *J. Rheology* **27** 201–10

Bercoff J, Tanter M, Muller M and Fink M 2004 The role of viscosity in the impulse diffraction field of elastic waves induced by the acoustic radiation force *IEEE Trans. Ultrason Ferr.* **51** 1523–36

Berry G P, Bamber J C, Armstrong C G, Miller N R and Barbone P E 2006 Towards an acoustic model-based poroelastic imaging method: I. Theoretical foundation *Ultrasound Med. Biol.* **32** 547–67

Biot M A 1941 General theory of three-dimensional consolidation *J. Appl. Phys.* **12** 155–64

Biot M A 1962 Mechanics of deformation and acoustic propagation in porous media *J. Appl. Phys.* **33** 1482–98

Blackstock D T 2000 *Fundamentals of Physical Acoustics* (New York: Wiley)

Britannica E 2013 *Ockham's razor* (www.britannica.com/EBchecked/topic/424706/Ockhams-razor)

Caputo M 1967 Linear models of dissipation whose q is almost frequency dependent-II *Geophys. J. R. Astr. Soc.* **13** 529–39

Carstensen E L and Parker K J 2014 Physical models of tissue in shear fields *Ultrasound Med. Biol.* **40** 655–74

Catheline S, Gennisson J L, Delon G, Fink M, Sinkus R, Abouelkaram S and Culioli J 2004 Measurement of viscoelastic properties of homogeneous soft solid using transient elastography: an inverse problem approach *J. Acoust. Soc. Am.* **116** 3734–41

Chan R W 2001 Estimation of viscoelastic properties of vocal-fold tissues based on time-temperature superposition *J. Acoust. Soc. Am.* **110** 1548–61

Chen S, Fatemi M and Greenleaf J F 2004 Quantifying elasticity and viscosity from measurement of shear wave speed dispersion *J Acoust Soc Am* **115** 2781–5

Chen S, Urban M W, Pislaru C, Kinnick R, Zheng Y, Yao A and Greenleaf J F 2009 Shearwave dispersion ultrasound vibrometry (SDUV) for measuring tissue elasticity and viscosity *IEEE Trans. Ultrason Ferr. Freq. Contr.* **56** 55–62

Chen S G *et al* 2013a Assessment of liver viscoelasticity by using shear waves induced by ultrasound radiation force *Radiology* **266** 964–70

Chen W and Holm S 2003 Modified Szabo's wave equation models for lossy media obeying frequency power law *J Acoust Soc Am* **114** 2570–4

Chen X, Shen Y Y, Zheng Y, Lin H M, Guo Y R, Zhu Y, Zhang X Y, Wang T F and Chen S P 2013b Quantification of liver viscoelasticity with acoustic radiation force: a study of hepatic fibrosis in a rat model *Ultrasound Med. Biol.* **39** 2091–102

Cheng S and Bilston L E 2007 Unconfined compression of white matter *J. Biomech.* **40** 117–24

de Boer R 1996 Highlights in the historical development of the porous media theory: toward a consistent macroscopic theory *Appl. Mech. Rev.* **49** 201–62

Delingette H 1998 Toward realistic soft-tissue modeling in medical simulation *P. IEEE* **86** 512–23

Doyley M M, Perreard I, Patterson A J, Weaver J B and Paulsen K M 2010 The performance of steady-state harmonic magnetic resonance elastography when applied to viscoelastic materials *Med. Phys.* **38** 3970–9 (PMID: 20879559)

Ehlers W and Markert B 2001 A linear viscoelastic biphasic model for soft tissues based on the theory of porous media *J. Biomech. Eng-T ASME* **123** 418–24

Fung Y C 1981 *Biomechanics: Mechanical Properties of Living Tissues* (New York: Springer) chapter 2

Gazit Y, Baish J W, Safabakhsh N, Leunig M, Baxter L T and Jain R K 1997 Fractal characteristics of tumor vascular architecture during tumor growth and regression *Microcirculation* **4** 395–402

Gennisson J L, Lerouge S and Cloutier G 2006 Assessment by transient elastography of the viscoelastic properties of blood during clotting *Ultrasound Med. Biol.* **32** 1529–37

Giannoula A and Cobbold R S C 2009 Propagation of shear waves generated by a modulated finite amplitude radiation force in a viscoelastic medium *IEEE Trans. Ultrason Ferr.* **56** 575–88
Graff K F 1975 *Wave Motion in Elastic Solids* (Oxford: Clarendon)
Grizzuti N, Buonocore G and Iorio G 2000 Viscous behavior and mixing rules for an immiscible model polymer blend *J. Rheology* **44** 149–64
Holm S and Nasholm S P 2014 Comparison of fractional wave equations for power law attenuation in ultrasound and elastography *Ultrasound Med. Biol.* **40** 695–703
Holm S, Näsholm S P, Prieur F and Sinkus R 2013 Deriving fractional acoustic wave equations from mechanical and thermal constitutive equations *Comput. Math. Appl.* **66** 621–9
Humphrey J D 2003 Continuum biomechanics of soft biological tissues *Proc. R. Soc. Lond. A* 3–46
Kiss M Z, Varghese T and Hall T J 2004 Viscoelastic characterization of *in vitro* canine tissue *Phys. Med. Biol.* **49** 4207–18
Koeller R C 1984 Applications of fractional calculus to the theory of viscoelasticity *J. Appl. Mech-T ASME* **51** 299–307
Konofagou E E, Harrigan T P, Ophir J and Krouskop T A 2001 Poroelastography: imaging the poroelastic properties of tissues *Ultrasound Med. Biol.* **27** 1387–97
Liu Z and Bilston L 2000 On the viscoelastic character of liver tissue: experiments and modelling of the linear behaviour *Biorheology* **37** 191–201
Mainardi F 1996 The fundamental solutions for the fractional diffusion-wave equation *Appl Math Lett* **9** 23–8
Mak A F 1986 Unconfined compression of hydrated viscoelastic tissues: a biphasic poroviscoelastic analysis *Biorheology* **23** 371–83 (PMID: 3779062)
Miller K and Chinzei K 1997 Constitutive modelling of brain tissue: experiment and theory *J. Biomech.* **30** 1115–21
Mow V C, Holmes M H and Lai W M 1984 Fluid transport and mechanical properties of articular cartilage: a review *J. Biomech.* **17** 377–94
Mow V C, Kuei S C, Lai W M and Armstrong C G 1980 Biphasic creep and stress relaxation of articular cartilage in compression? Theory and experiments *J. Biomech. Eng.* **102** 73–84
Parker K J, Doyley M M and Rubens D J 2011 Imaging the elastic properties of tissue: the 20 year perspective *Phys. Med. Biol.* **56** R1–R29
Perrinez P R, Kennedy F E, Van Houton E E W, Weaver J B and Paulsen K D 2009 Modeling of soft poroelastic tissue in time-harmonic MR elastography *IEEE Trans. Biomed. Eng.* **56** 598–608
Perrinez P R, Kennedy F E, Van Houton E E W, Weaver J B and Paulsen K D 2010 Magnetic resonance poroelastography: an algorithm for estimating the mechanical properties of fluid-saturated soft tissues *IEEE Trans. Med. Imaging* **29** 746–55
Righetti R, Ophir J, Srinivasan S and Krouskop T A 2004 The feasibility of using elastography for imaging the Poisson's ratio in porous media *Ultrasound Med. Biol.* **30** 215–28
Righetti R, Righetti M, Ophir J and Krouskop T A 2007 The feasibility of estimating and imaging the mechanical behavior of poroelastic materials using axial strain elastography *Phys. Med. Biol.* **52** 3241–59
Risser L, Plouraboue F, Steyer A, Cloetens P, Le Duc G and Fonta C 2007 From homogeneous to fractal normal and tumorous microvascular networks in the brain *J. Cerebr. Blood F. Met.* **27** 293–303
Robert B, Sinkus R, Larrat B, Tanter M and Fink M 2006 4J-3 a new rheological model based on fractional derivatives for biological tissues *Ultrasonics Symposium, 2006. IEEE* pp 1033–6
Samani A, Zubovits J and Plewes D 2007 Elastic moduli of normal and pathological human breast tissues: an inversion-technique-based investigation of 169 samples *Phys. Med. Biol.* **52** 1565–76
Sokolov I M, Klafter J and Blumen A 2002 Fractional kinetics *Phys. Today* **55** 48–54
Suki B, Barabasi A L and Lutchen K R 1994 Lung-tissue viscoelasticity: a mathematical framework and its molecular basis *J. Appl. Physiol.* **76** 2749–59 (http://jap.physiology.org/content/76/6/2749)
Sushilov N V and Cobbold R S C 2004 Frequency-domain wave equation and its time-domain solutions in attenuating media *J. Acoust. Soc. Am.* **115** 1431–6
Sutera S P 1993 The history of Poiseuille's law *Annu. Rev. Fluid. Mech.* **25** 1–19
Swartz M A and Fleury M E 2007 Interstitial flow and its effects in soft tissue *Annu. Rev. Biomed. Eng.* **9** 229–56
Szabo T L 1994 Time domain wave equations for lossy media obeying a frequency power-law *J. Acoust. Soc. Am.* **96** 491–500

Szabo T L 1995 Causal theories and data for acoustic attenuation obeying a frequency power-law *J. Acoust. Soc. Am.* **97** 14–24

Szabo T L and Wu J 2000 A model for longitudinal and shear wave propagation in viscoelastic media *J. Acoust. Soc. Am.* **107** 2437–46

Taylor L S 2002 Three-dimensional sonoelastography: principles and practices with applications to tumor visualization and volume estimation *Electrical & Computer Engineering* (Rochester, NY: University of Rochester)

Taylor L S, Lerner A L, Rubens D J and Parker K J 2002 A Kelvin-Voight fractional derivative model for viscoelastic characterization of liver tissue *ASME International Mechanical Engineering Congress and Exposition (New Orleans, LA)* pp IMECE2002-32605

Taylor L S, Richards M S and Moskowitz A J 2001 Viscoelastic effects in sonoelastography: impact on tumor detectability *Ultrasonics Symposium, 2001 IEEE* vol 2 pp 1639–42

Van Oene H 1978 *Polymer Blends* ed D R Paul and S Newman (New York: Academic) pp 295–352

Walker W F, Fernandez F J and Negron L A 2000 A method of imaging viscoelastic parameters with acoustic radiation force *Phys. Med. Biol.* **45** 1437–47

West G B, Brown J H and Enquist B J 1999 The fourth dimension of life: fractal geometry and allometric scaling of organisms *Science* **284** 1677–9

Zhang M, Castaneda B, Wu Z, Nigwekar P, Joseph J V, Rubens D J and Parker K J 2007 Congruence of imaging estimators and mechanical measurements of viscoelastic properties of soft tissues *Ultrasound Med. Biol.* **33** 1617–31